Title

Operando High-Energy-Resolution X-ray Spectroscopy of Evolving Cu Nanoparticle Electrocatalysts for CO2 Reduction

Journal

Journal of the American Chemical Society, 145(37)

ISSN

0002-7863

Authors

Feijóo, Julian
Yang, Yao
Guzman, Maria V Fonseca
et al.

Publication Date

2023-09-20

DOI

10.1021/jacs.3c08182

Peer reviewed

Supporting Information
Operando High-Energy-Resolution X-ray Spectroscopy of Evolving Cu Nanoparticle Electrocatalysts for CO_2 Reduction

Julian Feijóo,[1,2] Yao Yang,[1,2,3] Maria V. Fonseca Guzman,[1,2] Alfred Vargas,[4] Chubai Chen, [1,2] Christopher J. Pollock,[5] Peidong Yang[1,2,6,7]

[1]Department of Chemistry, University of California, Berkeley, CA 94720, USA.
[2]Chemical Sciences Division, Lawrence Berkeley National Laboratory, Berkeley, CA 94720, USA.
[3]Miller Institute for Basic Research in Science, University of California, Berkeley, CA 94720, USA.
[4]Department of Chemical and Biomolecular Engineering, University of California, Berkeley, CA 94720, USA.
[5]Cornell High Energy Synchrotron Source, Cornell University, Ithaca, NY 14853, USA.
[6]Department of Materials Science and Engineering, University of California, Berkeley, CA 94720, USA.
[7]Kavli Energy NanoScience Institute, Berkeley, CA 94720, USA.

This PDF file includes:

1. Materials and Methods
2. Discussions S1 and S2
3. Equations S1-S2
4. Tables S1-S6
5. Figures S1-S10

Experimental Section:

Chemicals and Materials

Trioctylamine (98%) (TOA) and tetradecylphosphonic acid (97%) (TDPA) were purchased from Sigma-Aldrich. Copper (I) acetate (97%) was purchased from Strem Chemicals. Potassium carbonate (99.997%, trace metals basis) was purchased from Alfa Aesar. Carbon paper (Sigracet 29AA) was purchased from Ion Power. Ag/AgCl electrodes were purchased from CH Instruments. Carbon dioxide (5.0 UHP) and Argon (5.0 UHP) gas were purchased from Praxair. Deionized water was from a Millipore system. All reagents were of analytical grade and used without further purification.

Synthesis of 5nm Cu Nanoparticles

Cu nanoparticles were synthesized as described in our previous work.[1]

TOA (10 mL) was purged with N_2 at 130 °C for 30 min. After cooling to room temperature, Cu(I) acetate (1 mmol) and TDPA (0.5 mmol) were added while stirring vigorously. The solution was heated to 180°C and kept there for 30 min under N_2. After cooling to room temperature, Cu-TDPA complex was collected as a light brown solid. The complex was washed with hexane (25 mL) and centrifuged at 5000 rpm for 15 min to remove TOA. This step was repeated two more times with 10 mL of hexane each. 10 mL of TOA were purged with N_2 at 130 °C for 30 minutes and then heated to 250°C. The Cu-TDPA complex was redispersed in 2 mL of 1-octadecene and injected into the hot TOA. The mixture was stirred at 250 °C for 30 min before allowing to cool to room temperature. Ethanol (30 mL) was added, followed by centrifugation at 6000 rpm for 15 minutes. The precipitated nanoparticles were split into two fresh centrifuge tubes, and each was washed twice with a mixture of chloroform (10 mL) and acetone (30 mL) followed by centrifugation at 12000 rpm for 10 minutes. Finally, the particles in each tube were redispersed in hexane (20 mL). Due to their tendency to aggregate, all experiments were conducted within a week of the synthesis of a particular batch of particles.

NP concentrations by mass of copper were measured by inductively coupled plasma optical emission spectroscopy on a Perkin Elmer ICP Optima 7000 DV Spectrometer.

Electrode Fabrication
Nanoparticles were dropcast onto 1 cm^2 of carbon paper electrodes and dried under vacuum. Electrochemical tests were conducted with loadings of 50 μg cm^{-2}. XAS measurements were repeated with higher loadings of 200 μg cm^{-2} for better signal quality.

Transmission Electron Microscopy
HAADF-STEM images were acquired on a Titan STEM at 300 keV with a convergence semi-angle of 21.4 mrad.

Operando High-Energy Resolution Fluorescence Detected X-ray Absorption Spectroscopy
All XAS data were collected at the PIPOXS beamline of the Cornell High-Energy Synchrotron Source (CHESS) under ring conditions of 100 mA at 6 GeV, using the home-made polyetheretherketone (PEEK) thin-liquid electrochemical cell (**Figure S3**). A Si(311) monochromator was used for energy selection of the incident x-rays while harmonic rejection and beam focusing was achieved using a pair of Rh-coated focusing mirrors. XES intensity was recorded using five Si(444) analyzer crystals (R = 85 cm) and a Pilatus 100K detector aligned in Rowland geometry. The space between the sample, analyzers, and detector was filled with He to reduce scattering of the emitted x-rays.
The spectra were normalized using PyMca and then imported to Athena for further analysis. EXAFS fitting was done in Artemis.
A Biologic SP-200 potentiostat was used for electrochemical measurements at the beamline.

Supplementary Discussions:

Discussion S1: EXAFS fitting
The EXAFS equation (Equation S2) shows that coordination number CN and amplitude reduction factor S_0^2 are dependent variables. S_0^2 is an experimental parameter specific for a certain beamline / setup and its value can be determined from the spectrum of a well-defined reference compound, such as a metal foil. With S_0^2 known, the CNs of materials of unknown structures can be determined. However, HERFD EXAFS has been reported to sometimes result in increased oscillation amplitude and intensity of R-space peaks compared to conventional EXAFS,[2] while HERFD of Cu foil suffers from self-absorption. Neither of these works well as a reference. Thus, we employed the steady-state metallic Cu as an internal reference for EXAFS fitting given the fully metallic state was verified by XANES analysis. We used the steady state spectrum to determine S_0^2 by assigning it a CN of 12 for face-centered cubic (fcc) Cu. The S_0^2 determined in this way was then held fixed for the other samples, and the CNs of Cu-Cu and Cu-O scattering paths were systematically varied to find the best fit. From table S1, it becomes apparent that there are two good fits with S_0^2 of 1.1 and 0.95, respectively. The former value was used for further analysis in the main text and in tables S2 and S3 based on the slightly better reduced χ^2 value and R-factor. The latter value with slightly improved Debye-Waller factor was also tested as shown in tables S4 and S5; the key messages of predominantly metallic character and low Cu-Cu CN within the accuracy of EXAFS remain the same regardless of the S_0^2 value used. For the 15-minute sample, there are two good fits; one fully metallic and the other including some Cu-O scattering contribution. Based on the small difference in the statistical parameters between these two fits it is not necessary to include the oxygen scattering, but neither can the presence of small amounts of Cu_2O at this timepoint be ruled out.
Data from k = 3 to k = 9 was used to convert to R-space. The fitting was then done in R-space with a fitting window of R = 1.3 to 3.0 for all fits.

Discussion S2: Expected average coordination number

The expected average coordination number for a nanoparticle should be a weighted sum of the bulk CN and surface CN. We used a Cu monolayer thickness of 0.21 nm to calculate the volume of the bulk core and surface monolayer of a 5 nm Cu NP. We then used these volumes to weigh the bulk and surface coordination numbers. The surface CN is a function of the size but is expected to be close to 8.5 on average for 5nm or larger.[3] For purely metallic 5nm nanoparticles, CN = 11.2 is expected. This should be the lower limit given that the particles tend to form larger aggregates during electrolysis, as can be seen in post-mortem SEM images (Figure S8). At a steady-state, CN of 12 is due to the dominant contribution from bulk Cu, while surface Cu is still present to contribute to catalysis. We propose undercoordinated surface Cu sites to be responsible, in accordance with the high multi-carbon selectivity from the stronger CO binding sites.

$$V_{core} = \frac{4}{3}\pi\left(\frac{d}{2} - 0.21\ nm\right)^3$$

$$V_{shell} = \frac{4}{3}\pi\left(\frac{d}{2}\right)^3 - V_{core}$$

$$CN_{average} = \frac{V_{core} * CN_{core} + V_{shell} \cdot CN_{shell}}{V_{core} + V_{shell}}$$

Equations:

$$F(\Omega,\omega) = \sum_f \left| \sum_n \frac{\langle f|T_2|n\rangle\langle n|T_1|g\rangle}{E_g - E_n + \Omega - \frac{i\Gamma_K}{2}} \right|^2 \cdot \frac{\frac{\Gamma_f}{2\pi}}{\left((E_g - E_f + \Omega - \omega\right)^2 + \frac{\Gamma_f^2}{4}} \quad \text{(S1)}[4]$$

(Energy bandwidth F, ground state g, intermediate state n, final state f, state energy E, transition operator T, lifetime-broadening Γ, incident energy Ω, emitted energy ω)

$$\Delta E = \sqrt{(\Delta t)^2 + (\Delta E_{Mono})^2} \quad \text{(S2)}$$

(Energy broadening ΔE, lifetime broadening Δt, monochromator resolution ΔE_{Mono})

Table S1. CO_2 electroreduction products and faradaic efficiencies of 5 nm Cu Nanoparticles.[1] The measurements were averaged over 3 independent trials.

	Product	**Faradaic Efficiency / %**
C_1	CO	10.36 ±2.22
	CH_4	0.14 ±0.12
	Formate	8.62 ±2.52
C_2	C_2H_4	35.17 ±3.45
	EtOH	11.96 ±2.42
	Acetate	0.91 ±0.16
	Acetaldehyde	0.24 ±0.05
C_3	Propanol	5.68 ±0.14
	Allyl Alcohol	0.59 ±0.08
	Acetone	0.09 ±0.02
	Propionaldehyde	0.35 ±0.06
Average Total C_{2+}		**55.0** ±4

Table S2. EXAFS fitting parameters for the steady state. Bold parameters were held fixed.

reduced χ2	R-factor	CN_{Cu-Cu}	CN_{Cu-O}	s_0^2	ΔE	ΔR_{Cu-Cu}	σ^2_{Cu-Cu}	ΔR_{Cu-O}	σ^2_{Cu-O}
67.8461691	0.0050004	**12**	**4**	1.2408649	6.6538100	-0.0047248	0.0125227	1.4287779	0.0234415
87.2217079	0.0064907	**12**	**3**	1.0959965	5.3903032	-0.0142583	0.0113814	0.5596304	0.1130558
87.4206532	0.0065034	**12**	**2**	1.0967252	5.3829514	-0.0143031	0.0113877	0.5532370	0.1075958
87.6734824	0.0065192	**12**	**1**	1.0978267	5.3723083	-0.0143680	0.0113971	0.5419504	0.1001169
87.3996047	0.0064849	**12**	**0.5**	1.1115551	5.1772485	-0.0156253	0.0115157	0.2118018	-0.0372790
88.0417359	0.0065407	**12**	**0.1**	1.1001054	5.3585882	-0.0144501	0.0114167	9.5276371	2.7757091
10.6556951	0.0065407	**12**	**0**	1.1001044	5.3585867	-0.0144501	0.0114167	/	/
7.4024358	0.0065407	**12**	**0**	**1.1001044**	5.3585758	-0.0144502	0.0114167	/	/
8.4773628	0.0075836	**12**	**0**	**1**	5.2675408	-0.0160487	0.0104598	/	/
9.5723436	0.0085966	**12**	**0**	**0.96**	5.2271079	-0.0167295	0.0100578	/	/
9.9123008	0.0089091	**12**	**0**	**0.95**	5.2167338	-0.0169029	0.0099554	/	/
12.0407370	0.0108555	**12**	**0**	**0.9**	5.1616712	-0.0178003	0.0094309	/	/

Table S3. EXAFS fitting parameters for the 30-minute sample using s02 = 1.1. Bold parameters were held fixed.

reduced χ2	R-factor	CN_{Cu-Cu}	CN_{Cu-O}	s_0^2	ΔE	ΔR_{Cu-Cu}	σ^2_{Cu-Cu}	ΔR_{Cu-O}	σ^2_{Cu-O}
38.2574121	0.0231517	**12**	**4**	**1.1**	8.3049848	0.0037714	0.0103722	-0.0601925	0.0714931
38.2547551	0.0231424	**12**	**3**	**1.1**	8.2942485	0.0037056	0.0103728	-0.0621147	0.0625464
38.2922871	0.0231530	**12**	**2**	**1.1**	8.2674152	0.0035363	0.0103729	-0.0631907	0.0504773
38.3816584	0.0231538	**12**	**1**	**1.1**	8.1963755	0.0030631	0.0103702	-0.0550132	0.0301560
36.8861900	0.0217519	**12**	**0.5**	**1.1**	7.9871340	0.0013523	0.0103083	-0.0180825	0.0027246
39.0660183	0.0239162	**12**	**0.1**	**1.1**	7.2680393	-0.0033941	0.0103880	-0.0192710	0.0000001
16.3779302	0.0256397	**12**	**0**	**1.1**	7.6816591	-0.0002825	0.0103701	/	/
15.7238975	0.0246564	**11.5**	**0**	**1.1**	7.6842298	-0.0006640	0.0099337	/	/
15.3007922	0.0240372	**11**	**0**	**1.1**	7.6864181	-0.0010587	0.0094832	/	/
15.1337711	0.0238212	**10.5**	**0**	**1.1**	7.6882410	-0.0014674	0.0090174	/	/
15.1322212	0.0238235	**10.45**	**0**	**1.1**	7.6884036	-0.0015091	0.0089699	/	/
15.1335453	0.0238302	**10.4**	**0**	**1.1**	7.6885625	-0.0015509	0.0089222	/	/
15.2514173	0.0240532	**10**	**0**	**1.1**	7.6897045	-0.0018912	0.0085347	/	/

Table S4. EXAFS fitting parameters for the 15-minute sample using s02 = 1.1. Bold parameters were held fixed.

reduced χ2	**R-factor**	**CN_{Cu-Cu}**	**CN_{Cu-O}**	**s_0^2**	**ΔE**	**ΔR_{Cu-Cu}**	**σ^2_{Cu-Cu}**	**ΔR_{Cu-O}**	**σ^2_{Cu-O}**
129.3406919	0.0708442	**12**	**4**	**1.1**	5.0285272	-0.0095781	0.0123138	0.0374426	0.0453215
131.8910928	0.0722065	**12**	**3**	**1.1**	4.9380902	-0.0100587	0.0123144	0.0350821	0.0397547
135.7721382	0.0742659	**12**	**2**	**1.1**	4.7953698	-0.0108219	0.0123125	0.0316429	0.0327653
142.6437670	0.0778697	**12**	**1**	**1.1**	4.4677328	-0.0126663	0.0123046	0.0232790	0.0233031
148.6758923	0.0809719	**12**	**0.5**	**1.1**	4.2003707	-0.0142000	0.0122943	0.0017469	0.0156092
154.7947806	0.0839045	**12**	**0.1**	**1.1**	3.6197897	-0.0177929	0.0123029	-0.0747242	0.0000000
62.3043224	0.0867238	**12**	**0**	**1.1**	3.6730484	-0.0173470	0.0123030	/	/
51.7516167	0.0718618	**11**	**0**	**1.1**	3.5833016	-0.0189555	0.0113379	/	/
41.8200324	0.0579038	**10**	**0**	**1.1**	3.4715086	-0.0207467	0.0103123	/	/
32.7567450	0.0451962	**9**	**0**	**1.1**	3.3599914	-0.0225927	0.0092132	/	/
24.8987779	0.0342169	**8**	**0**	**1.1**	3.2380387	-0.0245717	0.0080237	/	/
18.7161882	0.0256317	**7**	**0**	**1.1**	3.0939535	-0.0267732	0.0067203	/	/
14.8865803	0.0203985	**6**	**0**	**1.1**	2.9240569	-0.0292430	0.0052688	/	/
14.4434553	0.0199752	**5**	**0**	**1.1**	2.7537506	-0.0318736	0.0036151	/	/
19.0641582	0.0267396	**4**	**0**	**1.1**	2.5351465	-0.0350134	0.0016725	/	/
20.2193581	0.0109187	**6**	**0.5**	**1.1**	3.3859229	-0.0270761	0.0052002	-0.0370845	0.0042684
16.8911366	0.0091474	**6**	**1**	**1.1**	3.9049002	-0.0238115	0.0052174	-0.0260547	0.0147088
15.3434129	0.0083190	**6**	**1.5**	**1.1**	4.1318081	-0.0224548	0.0052326	-0.0199820	0.0221776
31.7864120	0.0170696	**7**	**0.5**	**1.1**	3.5739072	-0.0243776	0.0066677	-0.0419362	0.0052562
16.9202929	0.0093513	**5**	**0.5**	**1.1**	3.1852219	-0.0300297	0.0035217	-0.0297156	0.0030419
14.6025299	0.0080910	**5**	**0.8**	**1.1**	3.5295313	-0.0278559	0.0035405	-0.0286399	0.0096068
13.7069851	0.0076010	**5**	**1**	**1.1**	3.6865043	-0.0268833	0.0035502	-0.0276722	0.0132215
12.4785382	0.0069252	**5**	**1.5**	**1.1**	3.9390072	-0.0253589	0.0035672	-0.0249564	0.0206929
11.9083664	0.0066094	**5**	**2**	**1.1**	4.0663602	-0.0246190	0.0035779	-0.0223363	0.0266838
11.6123132	0.0064445	**5**	**2.5**	**1.1**	4.1480884	-0.0241616	0.0035843	-0.0197620	0.0316805

Table S5. EXAFS fitting parameters for the 30-minute sample using s02 = 0.95. Bold parameters were held fixed.

reduced χ2	**R-factor**	**CN_{Cu-Cu}**	**CN_{Cu-O}**	**s_0^2**	**ΔE**	**ΔR_{Cu-Cu}**	**σ^2_{Cu-Cu}**	**ΔR_{Cu-O}**	**σ^2_{Cu-O}**
34.9750404	0.0213017	**12**	**4**	**0.95**	8.3126098	0.0024448	0.0088884	-0.0735130	0.0667297
34.9184481	0.0212541	**12**	**3**	**0.95**	8.3041616	0.0023918	0.0088886	-0.0733697	0.0575371
34.8824698	0.0212102	**12**	**2**	**0.95**	8.2779361	0.0022214	0.0088882	-0.0708051	0.0451881
34.7699251	0.0210088	**12**	**1**	**0.95**	8.2015187	0.0016741	0.0088821	-0.0481033	0.0229893
31.0105580	0.0182638	**12**	**0.5**	**0.95**	7.8699968	-0.0009370	0.0087922	-0.0097099	0.0000000
38.8723235	0.0238380	**12**	**0.1**	**0.95**	7.6886833	-0.0015814	0.0088875	53.2969632	2.4956542
15.1363311	0.0238380	**12**	**0**	**0.95**	7.6886758	-0.0015814	0.0088875	/	/
15.6863827	0.0247842	**11**	**0**	**0.95**	7.6908043	-0.0023313	0.0080336	/	/
16.3460773	0.0258619	**10.5**	**0**	**0.95**	7.6914549	-0.0027257	0.0075844	/	/
17.2980056	0.0273986	**10**	**0**	**0.95**	7.6918199	-0.0031346	0.0071186	/	/
30.9078172	0.0182392	**11.5**	**0.5**	**0.95**	7.8606632	-0.0013913	0.0083687	-0.0087755	0.0000000
31.3938752	0.0185755	**11**	**0.5**	**0.95**	7.8370296	-0.0019521	0.0079329	-0.0071450	0.0000000
32.5198199	0.0192794	**10.5**	**0.5**	**0.95**	7.8616094	-0.0021823	0.0074863	-0.0050539	0.0000000
34.4101838	0.0204763	**10**	**0.5**	**0.95**	7.8589585	-0.0026205	0.0070222	-0.0049708	0.0000000

Table S6. EXAFS fitting parameters for the 15-minute sample using s02 = 0.95. Bold parameters were held fixed.

reduced $\chi 2$	R-factor	CN_{Cu-Cu}	CN_{Cu-O}	s_0^2	ΔE	ΔR_{Cu-Cu}	σ^2_{Cu-Cu}	ΔR_{Cu-O}	σ^2_{Cu-O}
89.1624095	0.0486872	**12**	**4**	**0.95**	4.9046359	-0.0120828	0.0106999	0.0259843	0.0425053
91.3296779	0.0498435	**12**	**3**	**0.95**	4.8241078	-0.0124973	0.0106989	0.0223850	0.0368699
94.6191646	0.0515880	**12**	**2**	**0.95**	4.6520372	-0.0134433	0.0106949	0.0166505	0.0297503
100.3835001	0.0546016	**12**	**1**	**0.95**	4.3409532	-0.0151963	0.0106821	0.0007407	0.0194171
104.6960610	0.0565090	**12**	**0.5**	**0.95**	3.7732928	-0.0189955	0.0106899	-0.0755470	-0.0020735
111.7023043	0.0603112	**12**	**0.1**	**0.95**	3.4601456	-0.0205428	0.0106862	-0.0644878	0.0000000
45.3458370	0.0628560	**12**	**0**	**0.95**	3.5098110	-0.0201043	0.0106930	/	/
37.1612367	0.0513671	**11**	**0**	**0.95**	3.4174970	-0.0216512	0.0097728	/	/
29.7385956	0.0409739	**10**	**0**	**0.95**	3.3154700	-0.0233044	0.0087922	/	/
23.3262858	0.0320267	**9**	**0**	**0.95**	3.2086024	-0.0250438	0.0077384	/	/
18.2583880	0.0250006	**8**	**0**	**0.95**	3.0738177	-0.0270203	0.0065953	/	/
14.9967608	0.0205455	**7**	**0**	**0.95**	2.9323080	-0.0291246	0.0053386	/	/
14.2079944	0.0196041	**6**	**0**	**0.95**	2.7812471	-0.0314010	0.0039342	/	/
16.9008822	0.0236030	**5**	**0**	**0.95**	2.6224330	-0.0338820	0.0236030	/	/
22.1334649	0.0124022	**5**	**0.5**	**0.95**	2.9251920	-0.0329580	0.0021981	-0.0215819	0.0001026
18.8431507	0.0105966	**5**	**1**	**0.95**	3.4179960	-0.0298559	0.0022445	-0.0267074	0.0097781
17.5783804	0.0098889	**5**	**1.5**	**0.95**	3.6853724	-0.0282126	0.0022660	-0.0276696	0.0168317
15.0977030	0.0083158	**6**	**0.8**	**0.95**	3.4588685	-0.0279709	0.0038572	-0.0298730	0.0076723
14.5528045	0.0080198	**6**	**0.9**	**0.95**	3.5493314	-0.0274050	0.0038616	-0.0291931	0.0094279
14.0961277	0.0077714	**6**	**1**	**0.95**	3.6255039	-0.0269305	0.0038658	-0.0285553	0.0110740
12.6385420	0.0069757	**6**	**1.5**	**0.95**	3.8970135	-0.0252725	0.0038825	-0.0254895	0.0181290
11.8974527	0.0065692	**6**	**2**	**0.95**	4.0405495	-0.0244250	0.0038939	-0.0228111	0.0238321

Supplementary Figures:

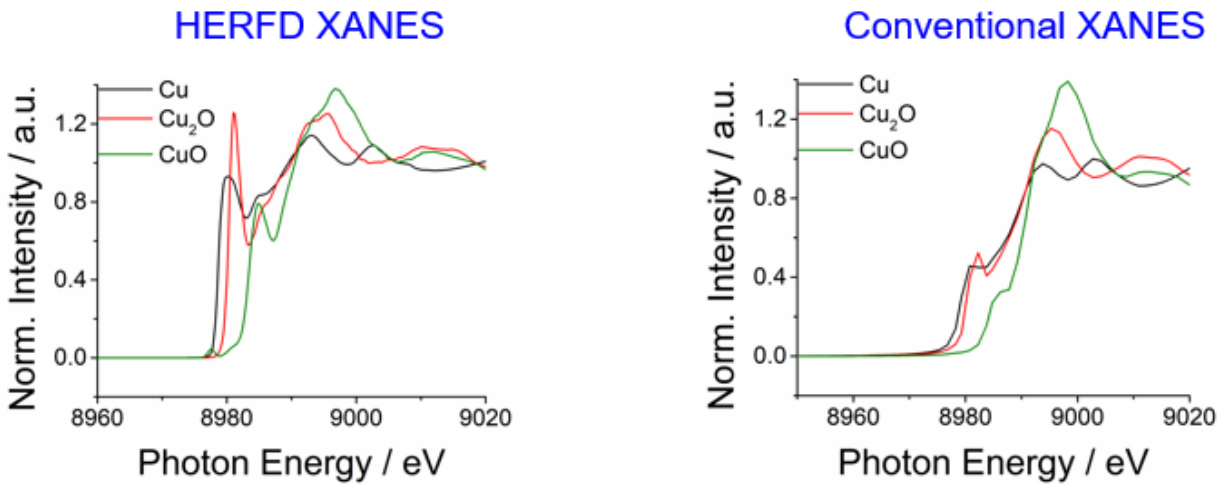

Figure S1. Comparison of different copper standards measured in HERFD and conventional XANES modes. HERFD XANES shows the pre-edge peak of CuO at 8977.6 eV, which was ascribed to the Jahn-Teller distortion and not resolvable in conventional XANES spectra.

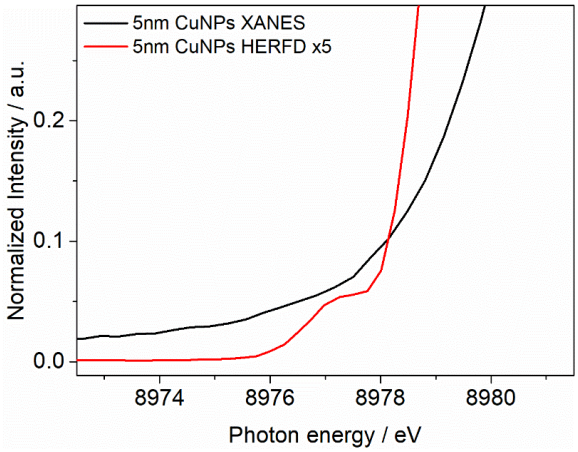

Figure S2. Comparison of conventional and HERFD XANES of 5nm Cu NPs at OCP. This illustrates that conventional XANES has a background intensity more than five times higher than the HERFD measurement. In addition to the improved energy resolution, this allows detection of the ligand peak in HERFD.

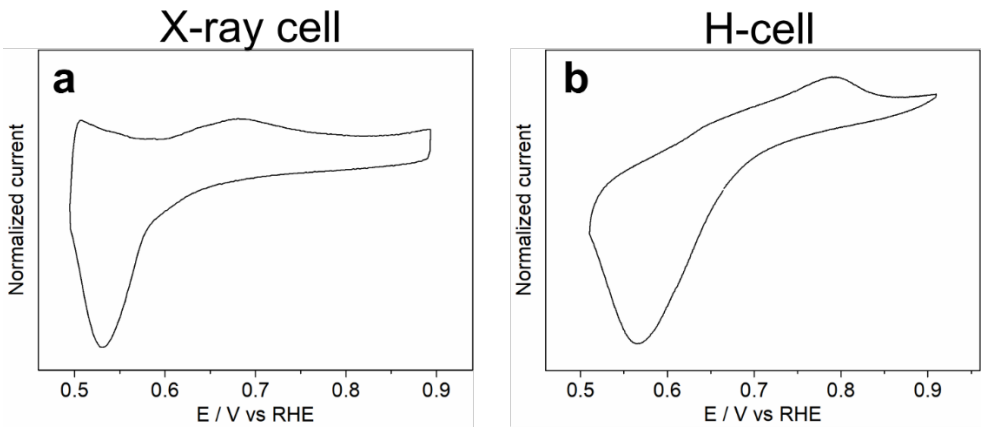

Figure S3. Cyclic Voltammograms of 5nm Cu NPs in a) the X-ray cell and b) an H-cell at 10 mV/s.

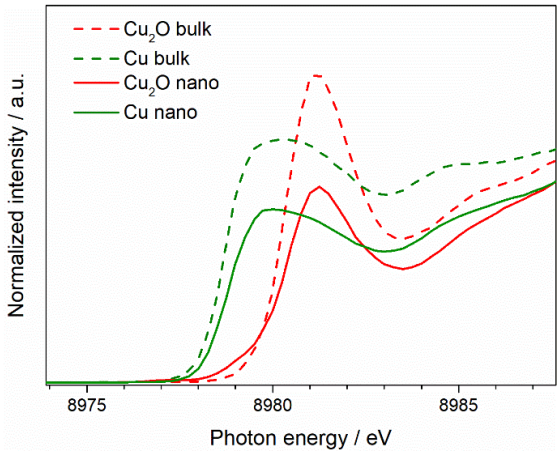

Figure S4. Comparison of HERFD-XAS spectra of bulk and nano-sized samples, showing the same edge energy for both bulk and nanoscale samples with a decreased pre-edge intensity of nano-sized samples.

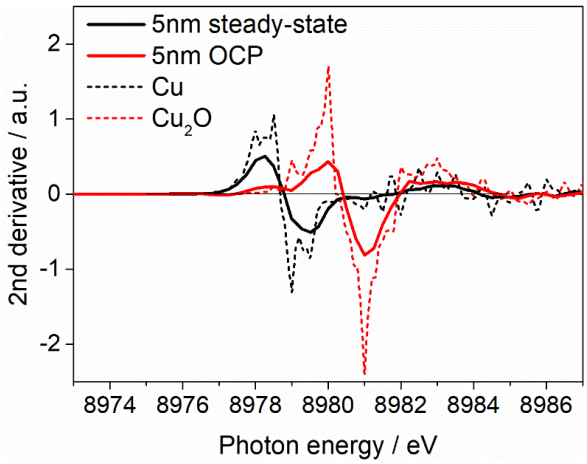

Figure S5. Comparison with nano-sized Cu standard shows that 5nm Cu NPs are fully metallic at the steady state.

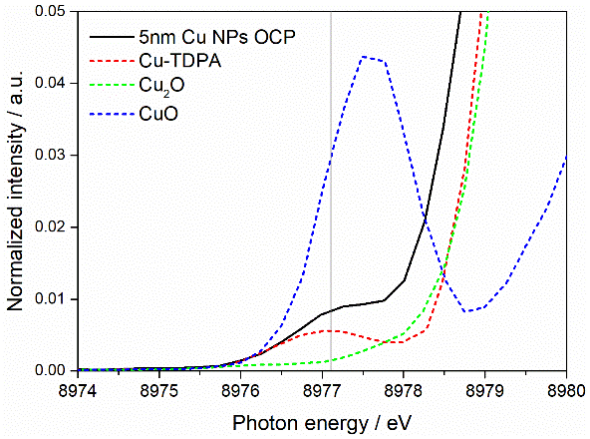

Figure S6. 5nm Cu NP ligand peak plotted with reference compounds showing good match to Cu-TDPA.

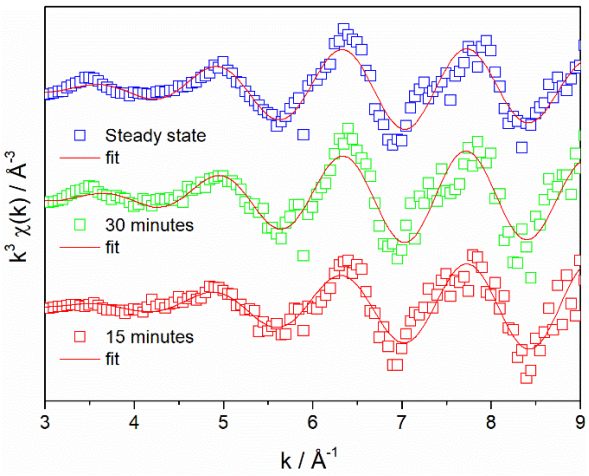

Figure S7. K-space EXAFS spectra and fits.

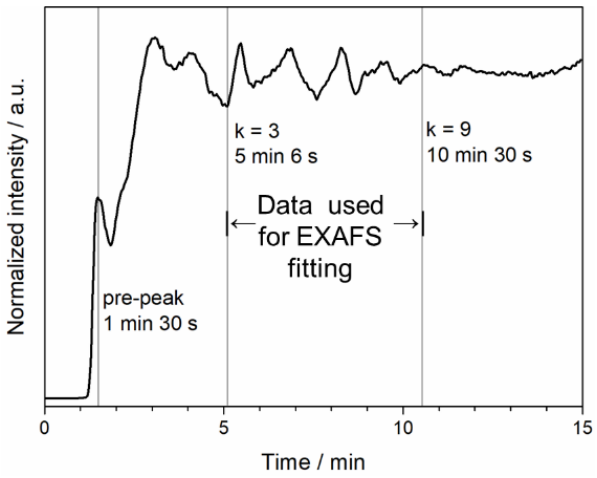

Figure S8. Visualization of the timescales over which the different regions of the XAS scan are recorded.

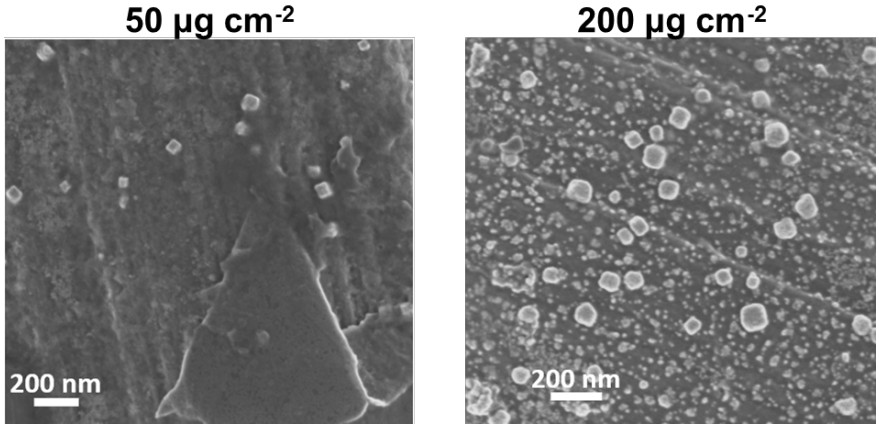

Figure S9. Post-electrolysis/XAS SEM of the electrodes with different mass loading of Cu NPs showing the formation of Cu_2O nanocubes upon air exposure. A loading of 50 µg cm^{-2} was often used for CO_2RR performance measurements while a higher loading of 200 µg cm^{-2} was used to achieve higher quality EXAFS spectra.

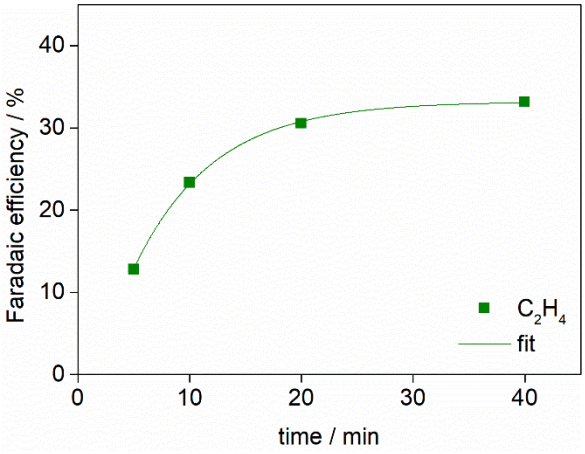

Figure S10. Representative C_2H_4 evolution trend in an H-cell at -0.8V vs. RHE. The selectivity initially increases sharply and reaches a steady state after about 20 minutes.

References

(1) Yang, Y.; Louisia, S.; Yu, S.; Jin, J.; Roh, I.; Chen, C.; Fonseca Guzman, M. V.; Feijóo, J.; Chen, P.-C.; Wang, H.; Pollock, C. J.; Huang, X.; Shao, Y.-T.; Wang, C.; Muller, D. A.; Abruña, H. D.; Yang, P. Operando Studies Reveal Active Cu Nanograins for CO2 Electroreduction. *Nature* **2023**, *614* (7947), 262–269. https://doi.org/10.1038/s41586-022-05540-0.

(2) Frenkel, A. I.; Small, M. W.; Smith, J. G.; Nuzzo, R. G.; Kvashnina, K. O.; Tromp, M. An *in Situ* Study of Bond Strains in 1 Nm Pt Catalysts and Their Sensitivities to Cluster–Support and Cluster–Adsorbate Interactions. *J. Phys. Chem. C* **2013**, *117* (44), 23286–23294. https://doi.org/10.1021/jp4062658.

(3) Reske, R.; Mistry, H.; Behafarid, F.; Roldan Cuenya, B.; Strasser, P. Particle Size Effects in the Catalytic Electroreduction of CO_2 on Cu Nanoparticles. *J. Am. Chem. Soc.* **2014**, *136* (19), 6978–6986. https://doi.org/10.1021/ja500328k.

(4) Glatzel, P.; Bergmann, U. High Resolution 1s Core Hole X-Ray Spectroscopy in 3d Transition Metal Complexes—Electronic and Structural Information. *Coordination Chemistry Reviews* **2005**, *249* (1–2), 65–95. https://doi.org/10.1016/j.ccr.2004.04.011.